International Journal of Current Engineering and Technology
E-ISSN 2277 – 4106, P-ISSN 2347 – 5161

Available at http://inpressco.com/category/ijcet

Research Article

Modelling of After Treatment Device for the Treatment of Exhaust from Spark Ignited Engine

Prasannakumar R S#* and Pratheeba C N^

#Central Electrochemical Research Institute, Karaikudi, Tamilnadu, India
^Anna University, Chennai, Tamilnadu, India

Received 30 May 2017, Accepted 31 July 2017, Available online 12 Aug 2017, **Vol.7, No.4 (Aug 2017)**

Abstract

Mobility plays a crucial role in a country's economy which offering threat to the environment. Therefore, vehicles that operate with low emissions are the need of the hour. This paper explains about the fundamental understanding of catalytic converter, (automotive pollution control device) and its operations. The pressure and velocity effect inside the catalytic converter is described by using the numerical model and then simulated. Catalytic converters help to reduce the harmful gases emission from the engine exhaust. The model was analysed by commercial CFD reproducing software FLUENT version 13.0.

Keywords: *Gas flow, Catalytic converter, Fluent, Exhaust, and Spark ignited engine, Air pollution, Pollution preventer*

1. Introduction

Air pollution is the biggest problem in Today's modernised world specifically automotive sectors. The emission from the motor vehicle engine contains lots of toxic gases such as Carbon monoxide, Nitrous Oxide and other unburnt Organic compounds (John B. Heywood, 1998). Pollution control devices play a significant role in the pollution prevention from engine exhaust. The catalytic converter is a device which is used for pollution prevention in engines (Ganesan. V., 2004) . It contains ceramic or metal substrate surface and the catalyst was coated on the surface of the substrate. That ceramic substrate was honeycomb structure with more flow passages (A.M.K. Mohiuddin *et al*, 2007).

In the ceramic substrate, the catalyst coated on the monolith walls which are inorganic oxides such as γ-Al_2O_3 (gamma alumina), CeO_2 (Ceria) and ZrO_2 (Zirconia). Noble metal catalyst, such as Platinum (Pt), Palladium (Pd) and Rhodium (Rh). The reactions varied with the type of the catalyst used in the catalytic converter. Most present day vehicles powered by gasoline fitted Three-way catalytic converter. Because of that catalytic converter, converts three major pollutants in the engine exhaust. Namely

- Carbon monoxide (CO_2)
- Unburned hydrocarbon (HC)
- Nitrous oxides. (NO)

*Corresponding author's ORCID ID: 0000-0003-3547-1761

The toxic gases like carbon Dioxide and Unburnt Hydrocarbon are undergoing catalytic combustion and the Oxides of nitrogen reduced back to Nitrogen. The catalytic converter efficiency is depending on the nature of flow inside the converter. The exhaust gas flow is a major factor, to determine the converter performance. So that the CFD modelling is a valuable tool to determine the efficient catalytic converter. In this work, ANSYS FLUENT used.

The toxic gases emission durability depends on catalyst coating quality. In CFD, the system consumes less memory space and less response time (PL.S. Muthaiah *et al*, 2010).

2. Methodology

In this paper the working fluid was Exhaust gas, and it has high Reynolds number. The equations of mass and momentum are solved using a SIMPLE algorithm to get velocity and pressure in the fluid domain. The assumption of an isotropic turbulence field employed in this turbulence model is valid for the current application (Koltsakis *et al*, 1997).

The conversion efficiency of the catalytic converter depends on various factors. On the one hand, there are the properties of the monolith such as a cross section of the monolith, the length of the monolith, the cell density of the monolith, wall thickness, wash coat formulation and loading.

2.1 Modelling pollutant formation

NO_x emission consists of mostly toxic gases and nitrous oxide (N_2O). The FLUENT NO_x model was a better

software code to analyse the pollutant forming mechanism (V.K. Chakravarthy *et al*, 2003). In this case, we use pressure based solver type for execution of the results. This solver type used for low-speed incompressible flows. The NO_x formation mechanisms are (Holmgren, T *et al*, 1997):

- Thermal NO_x formation - oxidation of atmospheric nitrogen present in the combustion air.
- Prompt NO_x formation - quick reactions at the flame front.
- Fuel NO_x formation - oxidation of nitrogen contained in the fuel
- Intermediate N_2O

2.2 Governing equations of No_x transport

The software code solves the mass transport equation of the NO species.

The general Global reactions for NO_x formation,

$$4NH_3 + 3O_2 \rightarrow 2N_2 + 6H_2O \quad (1)$$

$$4NH_3 + 6NO \rightarrow 5N_2 + 6H_2O \quad (2)$$

$$2NH_3 + NO_2 + NO \rightarrow 2N_2 + 3H_2O \quad (3)$$

This approach derived from the fundamental principle of mass conservation.

$$\frac{\partial}{\partial t}(\rho Y_{N_2o}) + \nabla(\rho \bar{v} Y_{N_2o}) = \nabla(\rho D Y_{N_2o}) + S_{N_2o}$$
$$\frac{\partial}{\partial t}(\rho Y_{NH_3}) + \nabla(\rho \bar{v} Y_{NH_3}) = \nabla(\rho D Y_{NH_3}) + S_{NH_3}$$
$$\frac{\partial}{\partial t}(\rho Y_{HCN}) + \nabla(\rho \bar{v} Y_{HCN}) = \nabla(\rho D Y_{HCN}) + S_{HCN}$$
$$\frac{\partial}{\partial t}(\rho Y_{NO}) + \nabla(\rho \bar{v} Y_{NO}) = \nabla(\rho D Y_{NO}) + S_{NO}$$

3. Modelling and simulation of a catalytic monolith

The greatest challenge for the catalytic reaction modeller is the knowledge of the reaction kinetics. In this thesis, we will focus on the heterogeneous surface reactions, since the homogeneous gas-phase reactions usually can be neglected in automotive catalytic converters due to the relatively low temperature, low pressure and short residence time. For the implementation of gas-phase chemistry, the interested reader referred to (Tsinoglou, D. N,2004).

A modified form of the Navier Stokes equation used to model the porous medium., which reduces to their classic shape and includes additional resistance terms induced by the porous region. The incompressible Navier-Stokes equations in a given domain Ω and time interval (0,t) can write as, (Loya, Sudarshan Kedarnath *et al*, 2011).

$$\rho\left[\frac{\partial u}{\partial t} + (u.\nabla)u\right] - \mu\nabla^2 u + \nabla p = f \text{on} \delta X(0,t)$$

$$\nabla u = 0 \; on \; \delta \; X \; (0,t)$$

Where, u = u(X,t) velocity vector

P = p(X,t) pressure field
μ = dynamic viscosity coefficient
f = external body forces acting on the fluid
The Reynolds number defined as (S.E. Voltz *et al* , 1973),

$$N_{Re} = \frac{\rho UL}{\mu}$$

Where, U – Characteristic velocity
L – Characteristic length
μ - viscosity

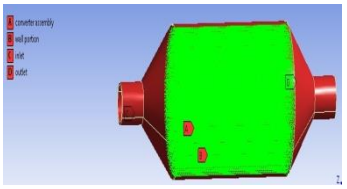

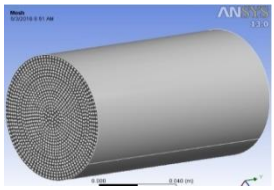

Fig.1 **Fig.2**

4. Preprocessing and processing

4.1 Problem detail

The catalytic converter model was developed by Ansys fluent. The Inlet and Outlet and Substrate portion identified.

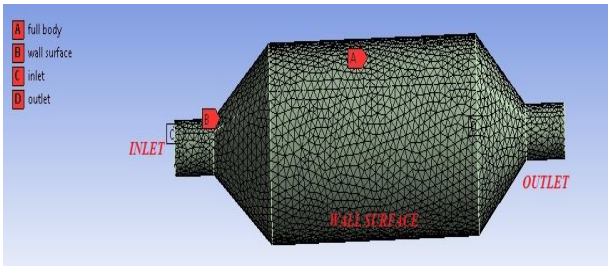

Fig.3

4.2 Problem formation

The catalytic converter modelled here shown in the figure. The exhaust gas flows in through the inlet with a velocity of 22.6 m/s, passes through the ceramic monolith substrate with circularly shaped channels, which are treated with noble metal catalysts (platinum & palladium) and then exits through the outlet. The constructed device meshed by using Hypermesh software which is in built in FLUENT. Tetrahedral type of mesh created.

4.3 Device geometry

Table 1

Device length	0.276 m
Device volume	7.8805E-05 m^3
Number of nodes	9906
Number of elements	37442
Analysis type	3D
Monolith Diameter	72mm
Monolith length	120 mm
Total length	276 mm
Wall thickness	30 mm
Monolith type	TWC – ceramic
Precious metals	Pt/Rh
Temperature range	500 – 900 ^{0}C

4.4 Initial processing steps

Before simulating the device the following preprocessing steps are carried out (Sampson *et al*, 1973).

Table 2

Pre processor	Solid works
Processor	Ansys fluent
Post processor	Ansys cfx & tecplot
Solver type	Pressure based solver
	Absolute velocity formulation
	Steady state period
Mesh quality	1. Minimum orthogonal quality = 5.14594E-01 2. Maximum aspect ratio = 8.2684
Reaction scheme	❖ Species transport model ❖ Volumetric reactions ❖ Laminar finite rate chemistry interaction
Volumetric species =8 (Reacting reagents)	H_2O, N_2, O_2, NH_3, NO, CO, CO_2, N_2O

4.4 Global reaction: NO_X reduction

$4NH_3 + 3O_2 \rightarrow 2N_2 + 6H_2O$
Slow SCR

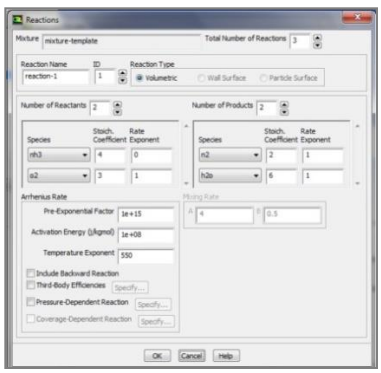

Fig .4

$4NH_3 + 6NO \rightarrow 5N_2 + 6H_2O$
Fast SCR

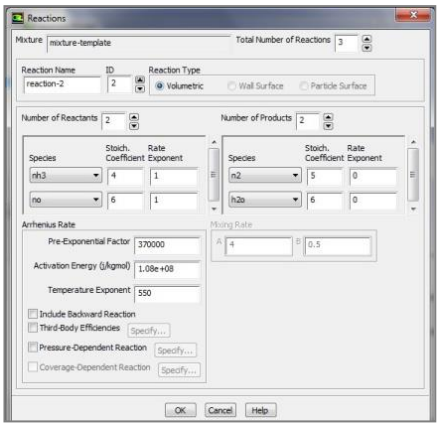

Fig.5

$2NH_3 + NO_2 + NO \rightarrow 2N_2 + 3H_2O$
Standard SCR

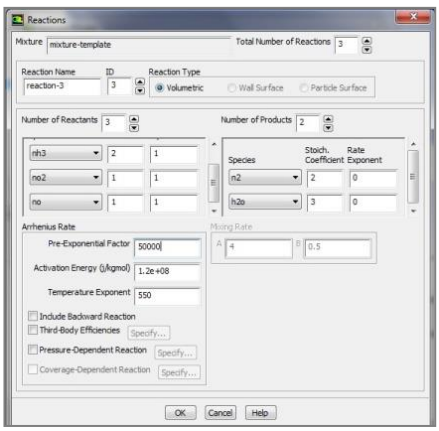

Fig.6

5. Results and Discussions

The designed converter device with the substrate portion uploaded into the ANSYS FLUENT for the simulation purpose. The initial processing already is done with the help of the preprocessing tool.

5.1 Contours of Static Pressure

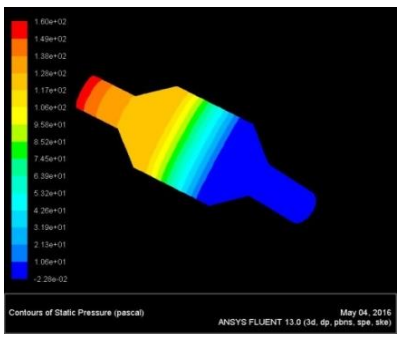

Fig.7

The above figure shows the pressure variation inside the device i.e. catalytic converter. Initially, the pressure is very high in the range of 159.52 Pascal. The pressure linearly reduced concerning the distance of the device in the range of 0.022 Pascal. It is meagre amount compared to initial level.

5.2 Contours of total temperature

This figure shows the total temperature distribution across the catalytic converter.

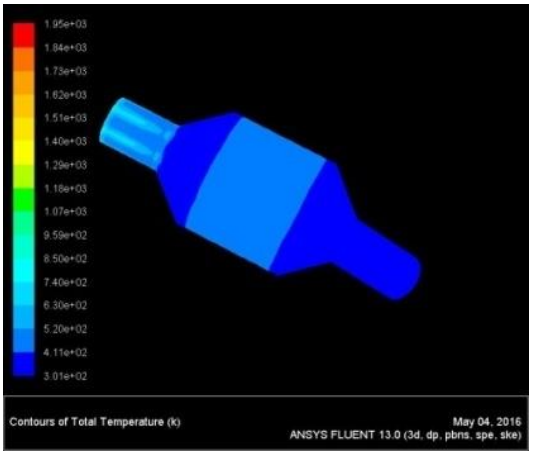

Fig.8

In substrate portion, the temperature distribution is in the range of 5.10E02. For the outlet portion it should have minimum temperature value 301.04 K compared to the initial temperature level.

5.3 Contours of wall temperature

Outer surface

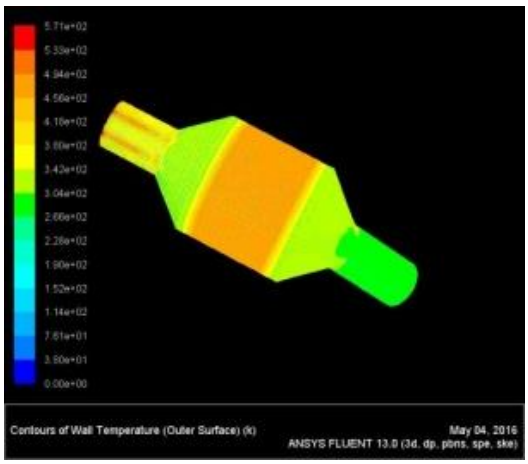

Fig.9

The above figure shows the outer surface wall temperature distribution in the catalytic converter. It shows the maximum temperature range of 570.56 K to minimum range of 0 K.

Inner surface

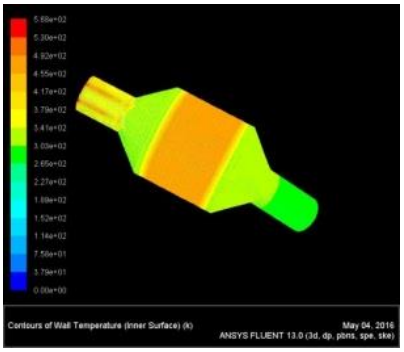

Fig.10

The above figure shows the temperature distribution on the inner surface of the catalytic converter. It demonstrates the variation of temperature in the maximum range of 568.16 K to a minimum range of 0 K.

5.4 Contours of internal energy

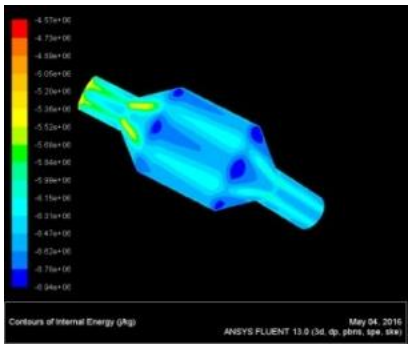

Fig.11

The above figure shows the internal energy contour of the catalytic converter. The energy varies from place to place, which is indicating the possibility of the reaction takes place. It varies in the range of -4.5E06 to -6.94E06

6. Contours of species

Mass fraction of H_2O

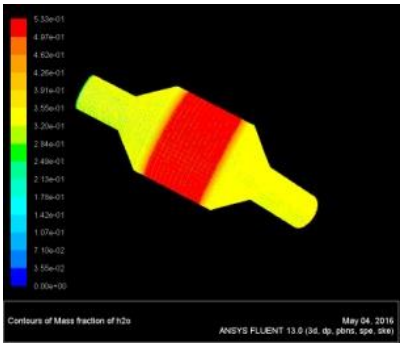

Fig.12

The above figure shows the mass fraction of water which formed as a product of the chemical reaction occurred in the chemical catalytic converter. The higher fractional amount is 0.53278.

Mass fraction of N_2

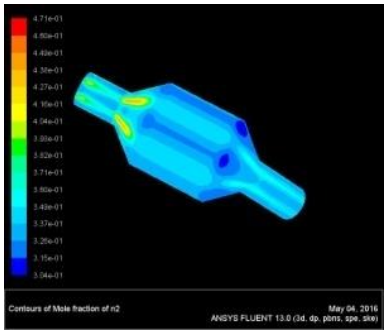

Fig.13

The above figure shows the nitrogen mass fraction values. The colour variation shows the fractional conversion of the nitrogen which is passed to the reactor i.e. catalytic converter. The conversion is in the range of 0.304 to 0.4714.

7. Static pressure at each location

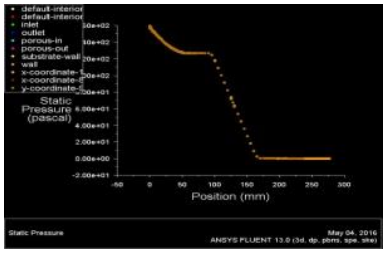

Fig.14

The above figure shows the variation of the pressure at each point of the overall length of the catalytic converter. Initially, the pressure range is very high in the range of 1.6E02 Pascal, and it gradually reduces the duration of the converter due to the expansion of area in substrate portion and minimum amount of major and minor losses of the pipe shape.

8. Mass Fraction: Nitrous Oxide

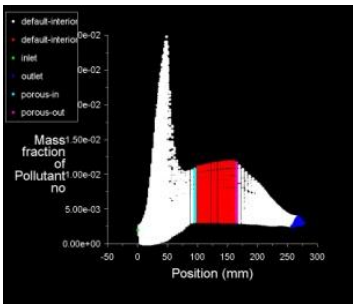

Fig.15

The above figure shows the mass fraction of pollutant Nitrous Oxide. Initially, the pollutant presenting value is too high. Throughout the length, due to NO_x reduction phenomena, the pollutant amount is gradually reduced and goes to the allowable value.

8. Validation of results

8.1 Validation of no conversion

The simulation carried out for the different temperature values. The obtained simulated results are validated the published literature values (Zukerman, R, 2009). The variation occurs in the simulated and published values. Those are because of the experimental condition and possibility of flow losses.

Table 3

Temperature	Experimental value	Simulated value
550	0.00298	0.00506
650	0.67881	0.8789
750	0.9614	0.9789
800	0.988	0.984

The graph is to be a plot between experimental values and corresponding simulated values. The temperature was taken on the X axis and the experimental and simulated values which taken on in the Y axis.

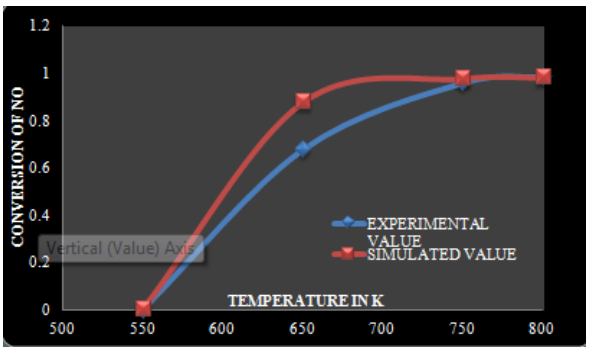

Fig.16

In the above the graph, 550^0 C is the light off temperature of the catalytic converter. Above that temperature, only the catalysts are got to be activated. The temperature gradually increased, and the conversion of NO to NO_2 always increased. The simulated values compare closely with experimental results.

8.2 Validation of amount of ammonia reacted

The simulation carried out for the different temperature values. The obtained simulated results are validated the published literature values (Zukerman, R, 2009). The variation occurs in the simulated and published values. Those are because of the experimental condition and possibility of possible flow losses.

Table 4

Temperature	Experimental value	Simulated value
550	0.0033	0.0027
600	0.0431	0.002
650	0.5601	0.49
700	0.8650	0.79
750	0.9623	0.85
800	0.9667	0.89

The graph is to be a plot between experimental values and corresponding simulated values (Tsinoglou *et al*, 2004). The temperature values are taken in X axis and Y axis, the experimental and simulated Ammonia conversion values taken. For the above graph, 550^{0}C is the light off temperature of the catalytic converter. With increasing temperature Ammonia conversion rate also increased. The simulated values compare closely with experimental results.

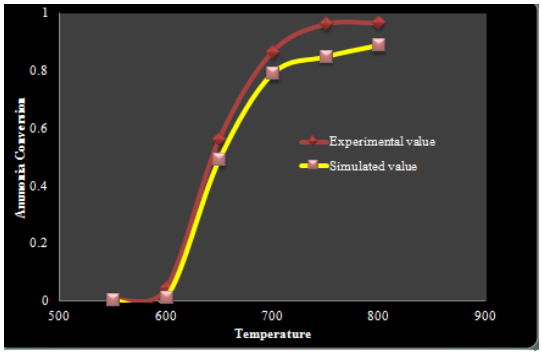

Fig.17

Conclusion

From the simulation done, the produced NO_x is reduced by injecting the reducing reagents like Ammonia. And the flow of the exhaust gas in a catalytic converter was analysed. And converter geometry was improved in the absence of exhaust gas recirculation and reduction of heat generation.

References

John B. Heywood (1998), Internal Combustion Engine Fundamentals,by McGraw-Hill Book Co, ISBN 0-07-100499-8.

Ganesan. V., (2004), Internal Combustion Engines, Second Edition, McGraw Hill.

A.M.K. Mohiuddin and Muhammad Nurhafez (2007), Experimental analysis and Comparison of Performance Characteristics of Catalytic Converters including Simulation, IJMME, vol.2, No.1,1-7.

Catalytic Converters (10 Jan 2011) International Platinum Group Metals Association

PL.S. Muthaiah, Dr.M. Senthil Kumar, Dr.S. Sendilvelan (October 2010), CFD Analysis of Catalytic Converter to Reduce Particulate Matter and Achieve Limited Back Pressure in Diesel Engine, GJRE, **2** Vol.10 Issue 5 (Ver1.0).

Gulati, S.T., 1995. Design of LFA Substrates, SAE Diesel Exhaust After treatment TOPTEC, Atlanta, GA, May 1995.

Koltsakis, G.C. and A.M. Stamatelos 1997 () Catalytic Automotive Exhaust After treatment. Progress in Energy and Combustion Science, Vol.23, pp.1-39.

V.K. Chakravarthy, J.C. Conklin, C.S. Daw, E.F. D'Azevedo (2003), Applied Catalysis A: General 241- 289.

Holmgren, T. Gronstedt, B. Andersson (1997), Reaction Kinetics and Catalysis Letters 60, 363.

S.E. Voltz, C.R. Morgan, D. Lieberman, S.M. Jacob (1973), Industrial & Engineering Chemistry Product Research and Development 12, 294.

Sampson, Robert E., and George S. Springer (1973) Effects of exhaust gas temperature and fuel composition on particulate emission from spark ignition engines. Environmental Science & Technology 7.1: 55-60.

M.Mansha , A.R.Saleem, Badar M Gauri, NaveedRamzan (2010)Development and testing of a detailed kinetic mechanism of natural gas combustion in internal combustion engine. Journal of natural gas chemistry 19,97 – 106.

Loya, Sudarshan Kedarnath (2011) Dynamic Incompressible Navier-Stokes Model of Catalytic Converter in 1-D Including Fundamental Oxidation Reaction Rate Expressions. Diss. University of Kansas.

Zukerman, R. (2009) Modelling and simulation of a smart catalytic converter combining NOx storage, ammonia production and SCR. Chemical Engineering Journal 155.1

Tsinoglou, Dimitrios N. (2004) Modelling of flow distribution during catalytic converter light-off. International journal of vehicle design 34.3

C. N. Satterfield (1980) Heterogeneous Catalysis in Practice. McGraw-Hill

Hsieh, Ming-Feng, and Junmin Wang (2011) Development and experimental studies of a control-oriented SCR model for a two-catalyst urea-SCR system. Control Engineering Practice 19.4: 409-422